

# SO<sub>2</sub> and NO<sub>x</sub> Removal from Combustion Flue Gas by Corona Discharge in Laboratory-Scale Experiment\*

Kazuo ONDA\*\*, Ken KATO\*\*\* and Yasuhiro KASUGA\*\*\*

It has been reported that SO<sub>2</sub> and NO<sub>x</sub> in flue gas can be removed by corona discharge and that pulsed corona discharge is as energy-efficient as electron-beam treatment. A large amount of data is required, however, to assess the industrial application of the corona discharge method to the removal of SO<sub>2</sub> and NO<sub>x</sub> from combustion flue gas. In this study experiments of SO<sub>2</sub> and NO<sub>x</sub> removal from actual and simulated combustion gas have been performed on a laboratory scale, where combustion gas composition, temperature, residence time in the discharge duct, and the polarity of high-voltage electrodes are changed for DC and pulsed corona discharge. The following experimental results are obtained: (1) the increase in H<sub>2</sub>O and O<sub>2</sub> concentration improves SO<sub>2</sub> and NO<sub>x</sub> removal rate, (2) dendritic (NH<sub>4</sub>)<sub>2</sub>SO<sub>4</sub> powders tend to deposit on high-voltage electrodes, and (3) the electrode polarity has a nominal effect on the removal rate under our experimental conditions.

**Key Words:** Environmental Engineering, Pollutant, Combustion Products, SO<sub>2</sub> and NO<sub>x</sub> Removal, Corona Discharge

## 1. Introduction

Acid rain is caused by the combustion of huge amounts of fossil fuels and by inadequate desulfurization and denitrification. Environmental pollution due to acid rain has become a subject of major concern worldwide. Japan, with its high level of development and relatively small land area, took comparatively early preventive measures against environmental pollution. Different countries have conducted extensive studies in order to develop more effective and economical methods for desulfurizing and denitrifying waste gas. A dry electron beam method is now being developed mainly in Japan and has been tested on a pilot-plant scale<sup>(1)</sup>. This method is said to enable desulfurization and denitrification as follows. Electrons

traveling at a high speed collide with flue gas molecules to form oxidation radicals such as OH, O, and HO<sub>2</sub> which, in turn, oxidize SO<sub>2</sub> and NO<sub>x</sub> into sulfuric and nitric acids. These acids are then neutralized by an alkali, such as NH<sub>3</sub>, and collected as fine ammonium sulfate and ammonium nitrate particles<sup>(2)</sup>. Small-scale experiments have demonstrated that such desulfurization and denitrification are caused by direct current<sup>(3)</sup> or pulsed corona discharge<sup>(4),(5)</sup>. Among other methods reported for desulfurizing and denitrifying flue gas using oxidation radicals, that using O<sub>3</sub>, which is produced by alternating current discharge along the surface, has been extensively studied<sup>(6)</sup>. Another process uses a H<sub>2</sub>O<sub>2</sub>-water solution<sup>(7)</sup>.

In desulfurization and denitrification tests using pulsed corona discharge with a pulse width of 1 μs or less, the discharge input per unit of the flue gas flow rate has been determined to be 10 to 50 J/g, which is nearly the same as that in the case of the electron beam method. Pulsed corona discharge is a highly efficient method for desulfurization and denitrification<sup>(8),(9)</sup> which suggests that in thermal power plants, flue gas can be desulfurized and

\* Received 23rd February, 1995. Japanese original: Trans. Jpn. Soc. Mech. Eng., Vol. 60, No. 575, B (1994), pp. 2607-2613. (Received 19th October, 1993)

\*\* Department of Electrical and Electronic Engineering, Toyohashi University of Technology, 1-1 Hibarigaoka, Tempaku, Toyohashi, Aichi 441, Japan

\*\*\* Energy Technology Division, Electrotechnical Laboratory, 1-1-4 Umezono, Tsukuba, Ibaraki 305, Japan

denitrified in a dry state using a small amount of the generated power. If the pulsed corona discharge is capable of such efficient desulfurization and denitrification in thermal power plants, it will significantly simplify the desulfurization and denitrification equipment more than the electron beam method, eliminating the need for countermeasures against radiation and improvement of power plant economy. We started desulfurization and denitrification tests using small-scale equipment to identify the features of pulsed corona discharge and to accumulate data required for its industrial use. Many discharge desulfurization and denitrification studies have been reported including experiments in air flows. Our objective is, however, to clarify the desulfurization and denitrification characteristics of flue gas by electric discharge. We limited target substances to actual flue gas or simulated combustion gas containing the main components of flue gas. We studied the following items using small-scale test equipment to determine factors governing desulfurization and denitrification by corona discharge, referring to previously reported data: direct current and pulsed discharge, polarity changes in high-voltage electrodes, actual and simulated combustion flue gas, changes in flue gas composition ( $H_2O$  and  $O_2$  concentration in particular), changes in flue gas temperature and residence time at the discharge duct, and deposits on the high-voltage electrode. This paper summarizes our experimental results.

## 2. Preliminary Experiments Using Combustion Gas

### 2.1 Combustion equipment and gas analysis

Preliminary experiments were conducted using city gas (13 A) and air. Combustion gas was generated using a premixed burner as shown in Fig. 1 and cooled by preheated water to the discharge duct temperature of 70–200°C in order to prevent water condensing on the duct wall. Honeycomb and mesh plates were provided at the duct entrance to obtain a uniform gas flow, and  $SO_2$ ,  $NO$ , and  $NH_3$  gases, each diluted with  $N_2$  gas to about 10% concentration, were supplied for the tests, where the concentrations of these gases were changed in such a way that the molarity of  $NH_3$  was the sum of two times the molarity of  $SO_2$  and the equal molarity of  $NO$ . The same concentrations of gases were used in the experiments in section 3. After passing through the discharge duct, the gas flowed through a vortex mixer, where the average concentration and temperature of the gas were measured.

$NO_x$  was measured using the chemiluminescence method and  $SO_2$  using the nondiffractive infrared

Table 1 Results of gas chromatography of combustion gas

Equivalence ratio $\phi$ (fuel/air)	Mass flow rate G (g/s)	Gas composition (dry mol %)						
		$O_2$	$N_2$	CO	$H_2$	$CH_4$	$CO_2$	Ar
1.05	2.06	0.55	81.54	1.89	1.62	0	12.45	0.97
	1.04	0.74	80.44	2.58	2.33	0.02	11.23	0.96
	0.52	2.16	76.77	3.88	1.29	1.31	8.50	0.92
1.00	2.06	0.80	81.89	1.19	0.96	0	12.14	0.98
	1.04	0.50	81.62	1.61	1.56	0.02	11.84	0.97
	0.52	3.07	77.12	4.15	1.13	1.40	7.85	0.90
0.95	2.05	1.30	81.84	0.54	0.60	0	12.12	0.98
	1.04	0.66	82.84	0.61	1.09	0	12.33	0.99
	0.52	1.74	80.90	2.73	0.90	0.45	9.76	0.97

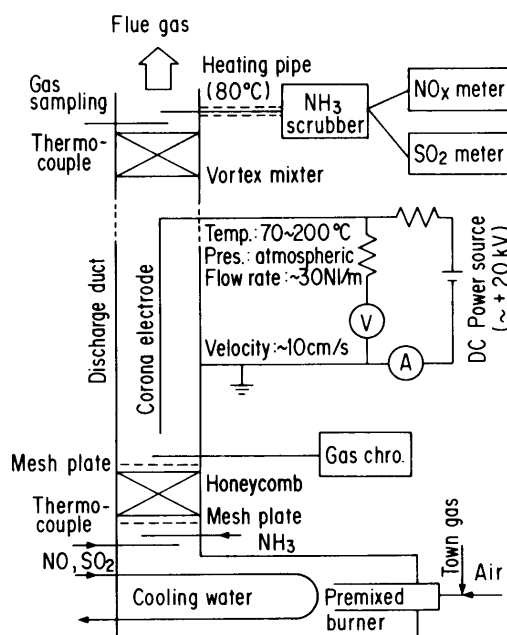


Fig. 1 Schematic diagram of corona discharge  $deSO_x$  and  $deNO_x$  test

absorption method. Combustion gas was sampled through a heating pipe to avoid water condensation, sent to a  $NH_3$  absorption scrubber containing phosphoric acid, and  $SO_2$  and  $NO_x$  concentrations were measured. The concentration of  $O_3$  at the duct outlet was measured by an ozone monitor using 254 nm wavelength ultraviolet absorption. Gas chromatography was used to analyze stable combustion gas compositions. Table 1 shows the results of gas chromatographic analysis under typical combustion conditions, where the equivalence ratio  $\phi$  (fuel/air) was kept approximately equal to 1, the value of an ideally mixed gas. At a combustion gas flow rate of 0.52 g/s, which is very low compared to the rated value of 2.06 g/s for the burner, residual  $O_2$  and unburned constituents of CO,  $H_2$ , and  $CH_4$  exist due to incomplete combustion.

### 2.2 $DeSO_x$ and $DeNO_x$ corona discharge ducts

Coaxial cylindrical ducts with high-voltage electrode wires placed in the center were used in most

desulfurization and denitrification experiments involving direct current corona<sup>(3),(10)</sup> and pulsed corona discharge<sup>(5),(9),(11)</sup>. However, in electrostatic precipitators dealing with large amounts of fuel gas, a number of wire electrodes are arranged parallel to the plate electrodes in the ducts<sup>(8)</sup>. We used a rectangular duct with three wire electrodes placed parallel to the gas flow as shown in Fig. 2. In discharge tests, the rectangular duct was grounded and a high voltage was applied to two types of wire electrodes, pins placed at right angles to plate electrodes and bars placed parallel to plate electrodes. Discharge gap  $d$  was changed in three steps from 1–3 cm to evaluate the effect of electric field strength using a power source of  $\pm 20$  kV. Because discharge occurred between the high-voltage electrode and the rectangular grounded duct, flue gas flowing through the duct center did not pass the discharge area, especially for a small discharge gap  $d$ . In corona discharge between plate and wire electrodes, a secondary flow was generated by the corona wind, thereby greatly enhancing heat transfer<sup>(12),(13)</sup>. The mixing caused by the secondary flow was thus anticipated to be very useful in promoting the  $\text{deSO}_x$  and  $\text{deNO}_x$  reaction. The outer surface of the discharge duct was heated to  $70^\circ\text{C}$  by electric heaters to prevent water condensation.

With the electric circuit used for the DC corona discharge test as shown in Fig. 1, a maximum voltage of  $+20$  kV or  $-20$  kV was applied to the high-voltage electrode through a load resistor. The discharge voltage was measured through a resistor divider and the current through a resistor connected to the ground line. Circuit parameters for our high-voltage pulse generator shown in Fig. 3 were selected as follows:

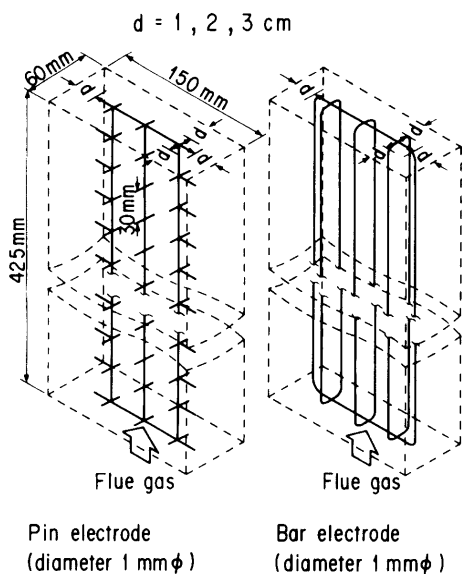


Fig. 2 Discharge duct and electrode configuration

first, the approximate value of capacitance  $C$  was chosen considering the capacity of the power source, then the values of the resistor  $R$  and the inductance  $L$  were tentatively determined so that the voltage pulse width was about  $1 \mu\text{s}$ . The voltage waveform was then measured at optimum circuit parameters. Probes for voltage and current measurement were set near the terminal for the duct to accurately measure the voltage and current supplied to the duct and to minimize the possible effects from the current flowing through the resistor  $R$ . The voltage and current waveforms recorded using a two-channel digital oscilloscope were transferred to a personal computer to calculate values such as power consumption.

Pulsed corona discharge requires less electrical power for desulfurization and denitrification than direct current corona discharge, since only electrons are considered to be accelerated by short pulse trains to collide with flue gas molecules and to produce oxidation radicals<sup>(9)</sup>. Direct current corona discharge tended to arc at high voltages. In pulsed corona discharge, however, where the voltage application is terminated before arcing, higher voltage and current are obtainable<sup>(4),(5),(11)</sup>.

### 2.3 Desulfurization and denitrification characteristics

$\text{SO}_2$  and  $\text{NO}_x$  concentrations were almost the same at the duct inlet and the outlet under no discharge. The concentration of  $\text{SO}_2$  was determined by the quantity of  $\text{SO}_2$  supplied at the duct inlet, while that of  $\text{NO}_x$  depended on the quantity supplied at the inlet plus the amount generated during combustion. Desulfurization and denitrification characteristics were obtained by measuring the change in the outlet concentration due to corona discharge. The voltage and current characteristics of direct current discharge for the two types of electrode, pin and bar, with a discharge gap of 1, 2, or 3 cm, tended toward high voltage (7.5 to 20 kV) for the bar electrode and high current (0.009 to 3.5 mA) for the pin electrode, together with a higher voltage with increasing

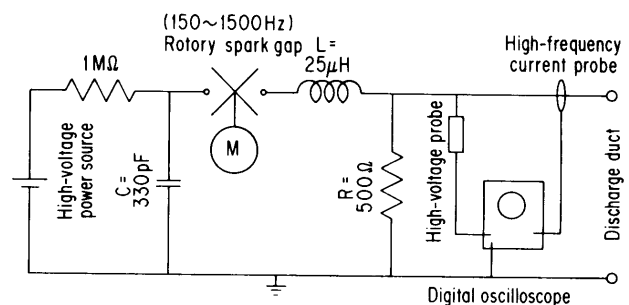


Fig. 3 Electrical circuit for high voltage pulse generation

discharge gap. With the  $\pm 20$  kV power source we used, the voltage and current characteristics for the discharge gap of 2 cm were stable over a comparatively wide range and the input power by discharge was large; thus most of the tests were conducted at a gap of 2 cm. In the transition from corona discharge to arcing, a large amount of  $\text{NO}_x$  was produced.

Figure 4 shows changes in concentrations of  $\text{SO}_2$  and  $\text{NO}_x$  at the outlet due to direct current or pulsed corona discharge, where the abscissa corresponds to a specific discharge input defined as consumed discharge power divided by mass flow of combustion gas. Desulfurization and denitrification rate cannot be arranged well in terms of discharge voltage or current. As in a number of previous studies<sup>(2)-(5)</sup>, the specific discharge input was adopted to evaluate these characteristics, which enabled the direct comparison of the results obtained by DC and pulsed corona discharges. Results of direct current corona discharge by pin electrodes and pulsed corona discharge by bar electrodes are shown in Fig. 4. Differences in the electrode type and in the polarity of high-voltage electrodes were small, partly because of the relatively low value of the specific discharge input. Desulfurization and denitrification rates were low at about 10 to 30%. Further studies applying higher voltage are required to determine parameters other than the specific discharge input.

Figure 5 shows denitrification characteristics in DC corona discharge for different gas flow rates  $G$  from 0.52 g/s to its rated value of 2.06 g/s at the equivalence ratio  $\phi$  of 1. Although initial concentrations of  $\text{NO}$  varied depending on the combustion gas flow rate because of the given supply amount of  $\text{NO}$ , a markedly improved denitrification was observed for a lower gas flow rate of about 0.5 g/s or for an increased residence time of the gas in the discharge

duct.

Previous studies showed a high desulfurization and denitrification rate in direct current corona with a specific discharge input of 100 to 400 J/g<sup>(3),(10)</sup>, and in pulsed corona with a specific discharge input of 10 to 50 J/g<sup>(5),(11)</sup>. In our experiments, such high desulfurization and denitrification rates could not be obtained due to the relatively low specific discharge input. Combustion gas composition was changed in our experiments, particularly the concentrations of unburned  $\text{H}_2$  and  $\text{CO}$ , in accordance with the combustion gas flow rate, as shown in Table 1. Previous studies on denitrification using electron beam<sup>(2)</sup> and pulsed corona discharge<sup>(11)</sup> showed that the denitrification process was improved by the presence of  $\text{CO}$  and  $\text{H}_2$ . Thus the presence of  $\text{CO}$ ,  $\text{H}_2$ , and  $\text{CH}_4$  might contribute to a high denitrification rate in Fig. 5 under a low flow rate ( $G=0.52$  g/s). Further studies are required, however, because the denitrification rate is insufficient, even though a certain amount of unburned components is found for  $G=1.04$  g/s.

In our experiments, it was difficult to obtain high desulfurization and denitrification rates, and experimental conditions changed with the amount of combustion gas flow. We therefore decided to conduct experiments based on simulated combustion gas, which have the advantages that specific discharge input can be increased and experimental parameters can be easily set. In DC corona discharge experiments, the outlet gas temperature was found to approach the setting temperature ( $75^\circ\text{C}$ ) by an electric heater soon after the start of discharge<sup>(14)</sup>, presumably due to the fact that heat transfer was enhanced by the secondary flow of the corona wind<sup>(12),(13)</sup> brought about by the discharge.

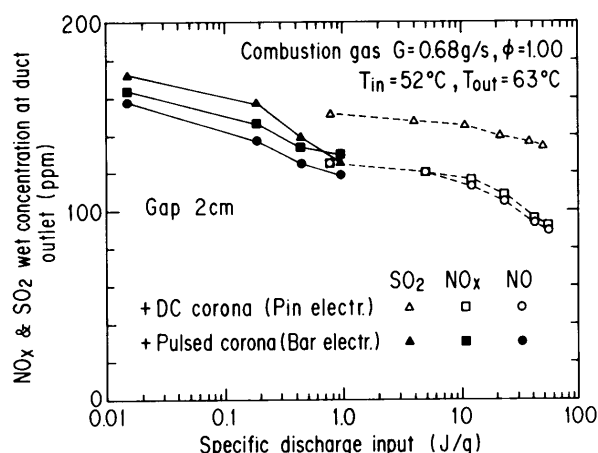


Fig. 4  $\text{SO}_2$  and  $\text{NO}_x$  concentration changes at the duct outlet due to specific discharge input

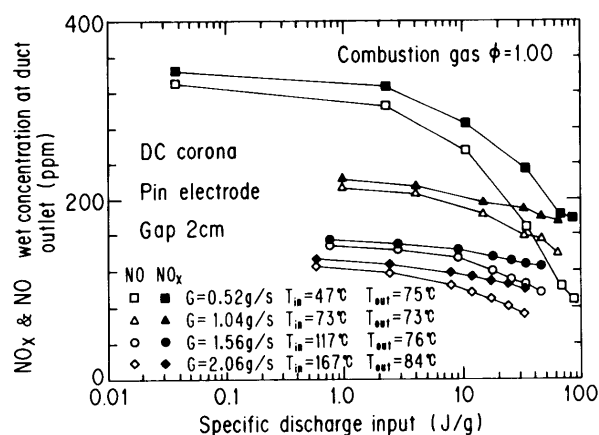


Fig. 5  $\text{NO}_x$  and  $\text{NO}$  concentration changes with various combustion gas flows

### 3. Desulfurization and Denitrification Experiments Using Simulated Combustion Gas

#### 3.1 Simulated combustion gas experiment

The schematic of the experimental apparatus is shown in Fig. 6. Combustion gas components  $N_2$ ,  $CO_2$ , and  $O_2$  are supplied in specified amounts from gas cylinders to the discharge duct through a heating pipe, while a measured amount of water was supplied to the duct through a special evaporator by electric heating. A simulated combustion gas mixed with  $SO_2$ ,  $NO$ , and  $NH_3$  was supplied to the discharge section after passing through a punch plate made of teflon to even out the gas flow.  $SO_2$  and  $NO_x$  concentrations were measured at the duct outlet. The entire duct, including a discharge space with a cross section of  $4 \times 8$  cm and 50 cm long, was heated by electric heaters to a maximum of  $150^\circ C$ . Three stainless steel wires with a diameter of 0.3 mm were used as high-voltage electrodes at the center of the duct and the discharge gap was set at 2 cm. City gas burnt with air containing residual oxygen of about 2% was assumed to be the simulated combustion gas. The gas analysis method and the power source were the same as those used in actual combustion gas experiments. When compared to the experiments in section 2, the gas flow rate selected was about 0.1 g/s, which was one-tenth of that in the previous section, while the residence time in the discharge section was prolonged to about 10 seconds. We confirmed that  $SO_2$  and  $NO_x$  concentrations at the inlet and outlet of the duct were nearly

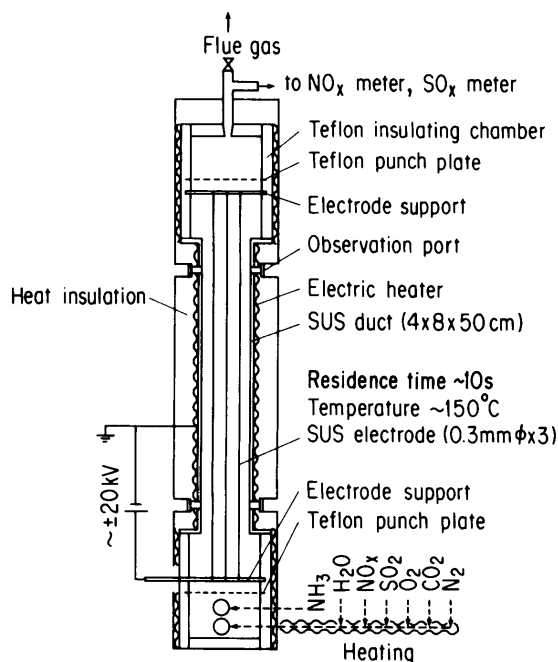


Fig. 6 Corona discharge de $SO_x$  and de $NO_x$  apparatus for simulated combustion gas

identical without discharge.

#### 3.2 Desulfurization and denitrification characteristics in DC and pulsed corona discharge

Typical desulfurization and denitrification characteristics in the DC corona discharge of simulated combustion gas ( $100^\circ C$ ) for both positive and negative polarities are shown in Fig. 7. The higher desulfurization and denitrification rates than the case before were attributable to the improvement in experimental conditions and higher specific discharge input. No marked difference was observed for both polarities. Specific discharge input should be reduced further to obtain similar desulfurization and denitrification results as reported in experiments<sup>(3),(10)</sup> with a coaxial cylindrical configuration of negative polarity. In many instances, the desulfurization rate was inferior to the denitrification rate, as found in the previous section. Voltages and current waveforms of DC corona discharge were recorded using a digital oscilloscope with a time resolution of 1  $\mu$ sec, and discharge power was calculated by taking the sum of the products of voltage and current for each segment, which corresponded well to the power (the product of DC voltage and current) measured using the setup shown in Fig. 1.

Typical desulfurization and denitrification characteristics in the pulsed corona discharge for both polarities are shown in Fig. 8, wherein a specific discharge input of about one-tenth that for DC corona discharge shown in Fig. 7 is found to be sufficient to obtain the same rates of desulfurization and denitrification. The negative polarity seemed to give better de $SO_x$  and de $NO_x$  characteristics as reported in previous studies<sup>(5),(11)</sup>, although only rough comparisons could be made because initial concentrations were slightly different. A marked improvement was observed in the de $SO_x$  and de $NO_x$  characteristics for

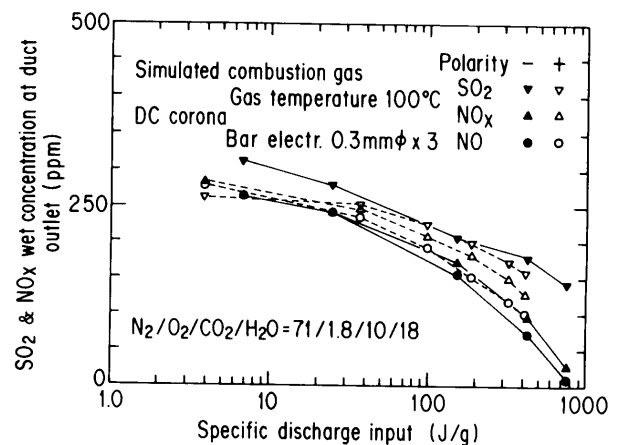


Fig. 7  $SO_2$  and  $NO_x$  concentration changes due to electrode polarity in DC corona discharge

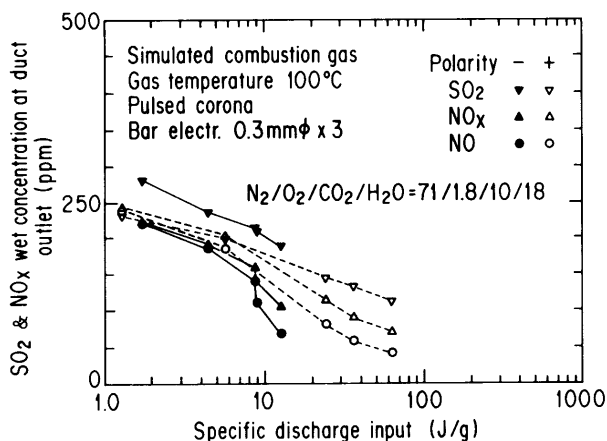


Fig. 8 SO<sub>2</sub> and NO<sub>x</sub> concentration changes due to electrode polarity in pulsed corona discharge

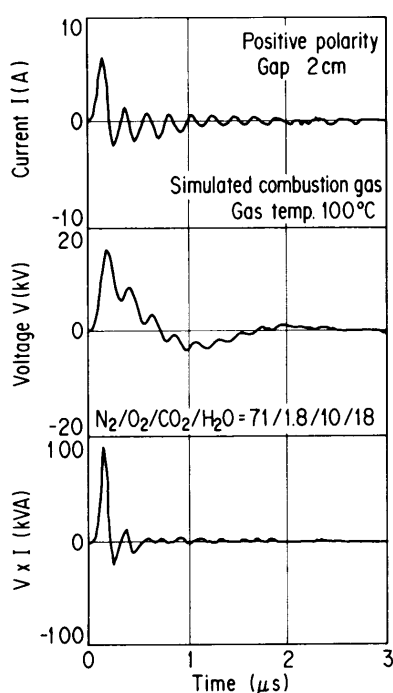


Fig. 9 Current and voltage pulse shapes in pulsed corona discharge

negative polarity around a specific discharge input of 10 J/g, although the reason for the change is not yet well understood. In experiments where gas temperatures were varied from 70 to 150°C, the desulfurization and denitrification characteristics were somewhat improved at lower temperatures, as in the case of the DC corona discharge. At increased gas flow rates, i.e., reduced gas residence times, the performance at the same specific discharge input deteriorated due to the reduced reaction time. Further studies are required, however, to determine the influence of temperature and gas residence time on performance.

A typical pulse waveform is shown in Fig. 9, which oscillates and has a half-width shorter than

1 μsec, i.e., 0.1 - 0.2 μsec. When the pulse width or the voltage applied was increased, arcing was observed at the discharge gap, at which time the voltage dropped and the current suddenly increased, and a large amount of NO<sub>x</sub> could be detected. Usually almost the same voltage waveform is observed. Average waveforms of voltage  $V$  and current  $I$  were recorded using a digital oscilloscope, and they were transferred to a personal computer to calculate the product waveform ( $V \times I$ ) as shown in Fig. 9. Thus, the energy per pulse multiplied by pulse repetition rate gives the discharge power. Instantaneous values of the voltage and current for the pulsed corona discharge turned out to be larger than those for the DC corona discharge, wherein the maximum values reached 17.6kV and 4.7mA, respectively. We found that when the pulse width of the voltage applied was reduced to a short enough time in order to prevent the occurrence of arcing, such a discharge condition would be preferable in desulfurization and denitrification. An experiment involving high-voltage electrodes with a diameter of 0.1 mm, instead of the original diameter of 0.3 mm, showed no substantial change in deSO<sub>x</sub> and deNO<sub>x</sub> characteristics, except that the thin electrodes tended to burn out due to excess current caused by arcing.

### 3.3 Changes in characteristics due to gas composition and deposits on electrodes

When combustion gas with air as an oxidizer is desulfurized or denitrified, no substantial change in the concentrations of N<sub>2</sub>, H<sub>2</sub>O, or CO<sub>2</sub> is observed. A change in the N<sub>2</sub> flow rate of 10 to 20% produces no significant changes in performance insofar as deSO<sub>x</sub> and deNO<sub>x</sub> data are arranged by the specific discharge input. The CO<sub>2</sub> concentration is about 10% under typical combustion conditions of fossil fuel. Even when this value is reduced to zero, performance remains almost the same with no meaningful change, insofar as deSO<sub>x</sub> and deNO<sub>x</sub> data are arranged by the specific discharge input. The reduction in the concentration of H<sub>2</sub>O degrades the performance, and a marked degradation of performance is observed in the absence of water vapor, as shown in Fig. 10. Although the O<sub>2</sub> concentration in combustion gas is usually small, i.e., 1.8% in our case, cessation of the O<sub>2</sub> supply also degrades desulfurization and denitrification characteristics, as shown in Fig. 11. These results agree well with numerical prediction based on a simulation model<sup>(15)</sup> where H<sub>2</sub>O and O<sub>2</sub> play an important role in pulsed corona discharge in the combustion gas. To date many experimental studies have been made on the removal of SO<sub>2</sub> and NO<sub>x</sub> from air flow. When the removal of SO<sub>2</sub> and NO<sub>x</sub> from combustion gas is intended, however, the concentrations of H<sub>2</sub>O and O<sub>2</sub>

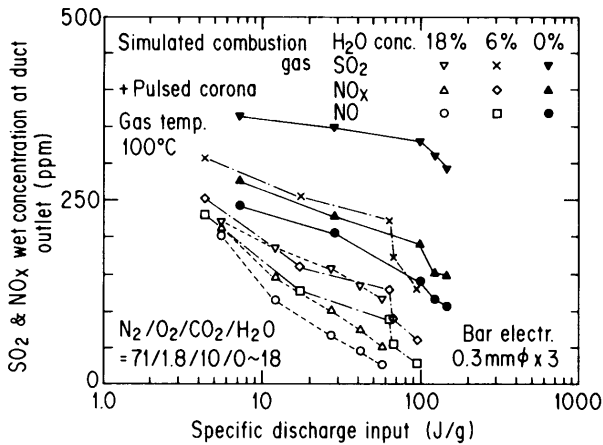


Fig. 10 SO<sub>2</sub> and NO<sub>x</sub> concentration changes by H<sub>2</sub>O addition

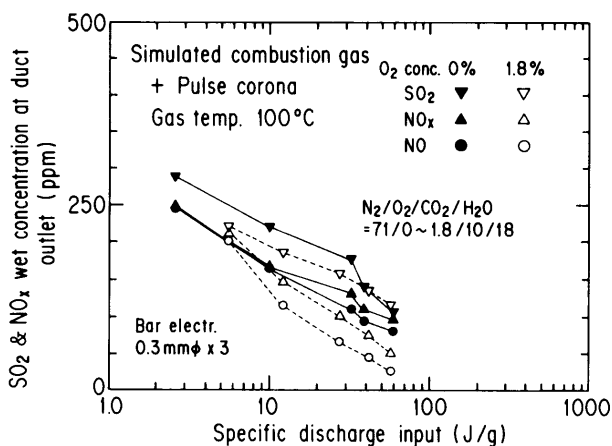


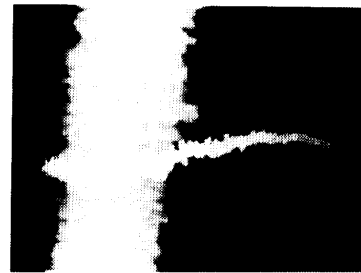
Fig. 11 SO<sub>2</sub> and NO<sub>x</sub> concentration changes by O<sub>2</sub> addition

are considered to be of primary importance. It is thus necessary to accumulate data from experiments, adopting the same composition as actual combustion gas.

In the experiment conducted at a gas temperature of about 100°C no notable change in the concentration of SO<sub>2</sub> and NO<sub>x</sub> at duct outlet was observed whether NH<sub>3</sub> was supplied or not. The initial stage of desulfurization and denitrification is assumed to involve an oxidation process by radicals such as OH generated by discharge, while NH<sub>3</sub> is considered to contribute to the neutralization of the produced acids, forming fine solid particles. In other words, if NH<sub>3</sub> is not added, SO<sub>2</sub> and NO are considered to be oxidized by the discharge to form sulfuric and nitric acids.

In accumulating further experimental data, it will be necessary to clarify the effect of NH<sub>3</sub> stoichiometry and of the SO<sub>2</sub> concentration on the deSO<sub>x</sub> and deNO<sub>x</sub> characteristics in the case of corona discharge, as in the case of the electron beam method<sup>(1),(16)</sup>. The improvement in denitrification char-

+ Pulsed corona Gas temp. 100°C  
Simulated combustion gas



N<sub>2</sub>/O<sub>2</sub>/CO<sub>2</sub>/H<sub>2</sub>O = 71/1.8/10/18

Fig. 12 Dendritic powder adhering to high-voltage electrodes in deSO<sub>x</sub> tests

acteristics by additions of small amounts of H<sub>2</sub> and CO<sup>(2),(11)</sup> will be confirmed in future experiments, wherein initial SO<sub>2</sub> and NO<sub>x</sub> concentrations will also be widely changed. Trials to measure the O<sub>3</sub> concentration at the duct outlet were made, but no meaningful value was obtained for direct current and pulsed corona discharges, since the O<sub>3</sub> monitor, which has a wide measurement range of up to 100 ppm, was also sensitive to SO<sub>2</sub>.

When the deSO<sub>x</sub> and deNO<sub>x</sub> process proceeds, white particles adhere to electrodes, although this fact does not seem to have been reported in any previous studies. Figure 12 shows the white powder adhering to a high-voltage electrode (SUS wire, 0.3 mm in diameter) after the desulfurization test. Deposited powder grew perpendicularly to the bar electrodes during discharge to form dendritic adhesion. After a few hours of continuous tests, the discharge voltage, current, and desulfurization and denitrification characteristics remained almost unchanged. Several types of tests were conducted to clarify the adhesion mechanism, i.e., a desulfurization test where SO<sub>2</sub> and NH<sub>3</sub> were added and a denitrification test where NO and NH<sub>3</sub> were added, wherein electrode polarities were changed both for direct current and pulsed corona discharges. In the desulfurization test, dendritic adhesion is observed as shown in Fig. 12, irrespective of the polarities and DC or pulsed corona discharge. In the denitrification test, however, much less adhesion is observed. X ray diffraction patterns of powder adhering to the high-voltage electrodes after desulfurization and denitrification tests are almost identical to those of (NH<sub>4</sub>)<sub>2</sub>SO<sub>4</sub> powder. Ion chromatographic analysis of an aqueous solution of the powder demonstrates that the powder contains 84 mol% of (NH<sub>4</sub>)<sub>2</sub>SO<sub>4</sub> and 16 mol% of NH<sub>4</sub>NO<sub>3</sub>. In a simultaneous desulfurization and denitrification test, the

Table 2 Comparison of specific discharge inputs for various deSO<sub>x</sub> and deNO<sub>x</sub> processes, and other processes

Item		Specific input
E-beam deSO <sub>x</sub> , deNO <sub>x</sub>	(1,2)	10~50J/g
DC corona deSO <sub>x</sub> , deNO <sub>x</sub>	(3,10)	100~400J/g
Pulsed corona deSO <sub>x</sub> , deNO <sub>x</sub>	(5,8,11)	10~50J/g
Electrostatic precipitator	(3)	2~8J/g
Heat transfer enhancement by corona wind	(12,13)	0.1~0.2J/g

adhered powder also consists mainly of (NH<sub>4</sub>)<sub>2</sub>SO<sub>4</sub>.

### 3.4 Comparison of specific discharge input

Specific discharge inputs reported previously for various desulfurization and denitrification processes using electron beam and corona discharge are given in Table 2. Further investigation is necessary, however, because these tests were not necessarily conducted under the same conditions, resulting in some variations in the specific discharge input for each test. The specific discharge input for the electron beam and the pulsed corona processes is found to be almost identical, i.e., 10 to 50 J/g. For DC corona discharge, the input is in the range of 100 to 400 J/g, which is one order of magnitude higher than that for the electron beam and pulsed corona discharge. The same values have been obtained from our experiment, although further improvement is necessary. The specific discharge input for electrostatic precipitators is one order of magnitude smaller than that for the pulsed corona discharge as shown in Table 2, and the specific discharge input for heat transfer enhancement by the corona wind is one order of magnitude smaller than that for electrostatic precipitators. In our experiments, the vertical main gas flow is assumed to be affected by the secondary flow caused by corona wind perpendicular to the main flow, which promotes the mixing of oxidizing radicals with combustion gas and results in improved deSO<sub>x</sub> and deNO<sub>x</sub> reaction.

Combustion gas of fossil fuels such as coal, oil and natural gas burned with about 5% excess air has an enthalpy of about 2700 J/g based on the high heating value. This enthalpy is converted to a specific electrical energy of 1080 J/g in a power generating system with 40% efficiency, which means that the specific discharge inputs of 10 to 50 J/g in the preceding electron beam and pulsed corona methods correspond to 1 to 5% of the generated power. In actual applications, however, these percentages must still be divided by the conversion efficiency of power sources for electron beam and pulsed corona methods. Overall system efficiency can only be evaluated when necessary data have been accumulated because the

conversion efficiency varies depending on the individual equipment and scale. The electron beam and pulsed corona methods have a drawback in that the power consumption is higher than that in conventional deSO<sub>x</sub> and deNO<sub>x</sub> methods. Further research and development is therefore needed to reduce the power consumption. With the problem of acid rain and increasing attention being paid to deSO<sub>x</sub> and deNO<sub>x</sub> technologies by electron beam and discharge methods<sup>(17)</sup>, great hopes are placed on the advancement of these new technologies.

### 4. Conclusion

Experimental laboratory-scale studies on dry simultaneous desulfurization and denitrification of combustion gas by direct current and pulsed corona discharge have been conducted in a duct provided with a pair of plate electrodes and parallel wire electrodes, where secondary flow caused by the corona wind is expected to promote mixing. In these experiments, the polarity of the high-voltage electrodes, gas flow rates, gas temperature, and gas compositions have been varied, and it has been found that the specific discharge input per unit of combustion gas flow in pulsed corona discharge is one order of magnitude lower than that in DC corona discharge as reported in previous studies in order to achieve the same desulfurization and denitrification rates. In addition, the following results have been obtained. (1) In experiments on the desulfurization and denitrification of combustion gas, the higher the water vapor and oxygen concentrations are, the higher the desulfurization and denitrification rates are. (2) Ammonium sulfate produced in the deSO<sub>x</sub> and deNO<sub>x</sub> reaction tends to be deposited on high-voltage electrodes in dendritic form, but ammonium nitrate deposits are few. (3) To obtain a high desulfurization and denitrification rate, specific discharge input must exceed a certain threshold, but the polarity change in high voltage electrodes has no significant influence.

Further investigation of the basic mechanisms of desulfurization and denitrification is necessary to clarify how radicals are produced in corona discharge under different conditions, how SO<sub>2</sub> and NO<sub>x</sub> are oxidized in the flow and temperature fields of the discharge duct, and how they react with alkaline materials to form particulate salts.

### Acknowledgment

We thank all who supported our studies by preparing the test apparatus and providing power source and measurement instruments.

## References

- (1) Frank, N.W. and Kawamura K., Final Report for Testing Conducted on the Ebara E-Beam Flue Gas Treatment System Process Demonstration Unit at Indianapolis, DOE Contract # AE 22-83 PC 6025 (1988).
- (2) Tokunaga, O. and Suzuki, N., Radiation Chemical Reactions in NO<sub>x</sub> and SO<sub>2</sub> Removal from Flue Gas, *Radiat. Phys. Chem.*, Vol. 24, No. 1 (1984), p. 145.
- (3) Ohtsuka, K., Yukitake, T. and Shimoda, M., Oxidation Characteristics of Nitrogen Monoxide in Corona Discharge Field, *Seidenki-Gakkaishi*, (in Japanese), Vol. 9, No. 5 (1985), p. 346.
- (4) Mizuno, A., Clements, J.S. and Davis, R.H., A Method for the Removal of Sulfur Dioxide from Exhaust Gas Utilizing Pulsed Streamer Corona for Electron Energization, *IEEE Trans. Ind. Appl.* Vol. IA-22, No. 3 (1986), p. 516.
- (5) Urabe, T., Wu, Y., Ono, M. and Masuda, S., Experimental Studies on NO<sub>x</sub> and SO<sub>x</sub> Removal by Pulse Corona Discharge, *Seidenki-Gakkaishi* (in Japanese), Vol. 12, No. 5 (1988), p. 354.
- (6) Namba, H., Suzuki, N. and Tokunaga, O., Removal of SO<sub>x</sub> and NO<sub>x</sub> in Coal-Fired Flue Gas by the Addition of Ozone and Ammonia, *JAERI-M 89-177* (in Japanese) (1989).
- (7) Soldavini, H., Vollständige SO<sub>2</sub>-Beseitigung aus Abgasen, *Chem. Analagen Verfahren*, Vol. 24, No. 11 (1991), p. 17-21.
- (8) Dinelli, G., Civitano, L. and Rea, M., Industrial Experiments on Pulse Corona Simultaneous Removal of NO<sub>x</sub> and SO<sub>2</sub> from Flue Gas, *Proc. 23rd. Annu. Meet. IEEE Ind. Appl.*, Vol. 2, (1988), p. 1620.
- (9) Masuda, S., Pulse Plasma Chemical Reaction, *Seidenki-Gakkaishi* (in Japanese), Vol. 14, No. 6 (1990), p. 473.
- (10) Ohtsuka, K., Yukitake, T. and Shimoda, M., Removal of SO<sub>2</sub> and NO from Flue Gas Using Wet Electrostatic Precipitators, *Seidenki-Gakkaishi* (in Japanese), Vol. 9, No. 5 (1985), p. 352.
- (11) Urabe, T., Wu, Y., Ono, M. and Masuda, S., Oxidation Characteristics of NO and SO<sub>2</sub> in Exhaust Gas from Municipal Refuse Incinerator by Pulse Corona Discharge, *J. Japan Soc. Air Pollut.* (in Japanese), Vol. 23, No. 4 (1988), p. 191.
- (12) Tada, Y., Takimoto, A., Ueda, D. and Hayashi, Y., Heat Transfer Enhancement in a Convective Field with Corona Discharge (Experimental Study for Parallel Wire-Electrode Arrangement), *Trans. Jpn. Soc. Mech. Eng.*, (in Japanese), Vol. 57, No. 533, B (1991), p. 217.
- (13) Tada, T., Takimoto, A., Ueda, D. and Hayashi, Y., Heat Transfer Enhancement in a Convective Field with Corona Discharge (Analytical Study for a Parallel Wire-Electrode Arrangement), *Trans. Jpn. Soc. Mech. Eng.*, (in Japanese), Vol. 57, No. 533, B (1991), p. 223.
- (14) Onda, K., Kasuga, Y. and Kato, K., NO<sub>x</sub> Removal Experiment from Combustion Gas by Corona Discharge, *Proc. 28th Symp. Comb. Japan* (in Japanese), (1990), p. 137.
- (15) Gallimberti, I., Impulse Corona Simulation for Flue Gas Treatment, *Pure Appl. Chem.*, Vol. 60, No. 5 (1988), p. 663.
- (16) Aoki, S., Electron-beam Flue Gas Treatment, *Nenryo-Kyokaishi*, (in Japanese), Vol. 69, No. 3 (1990), p. 165.
- (17) Penetrante, B.M., Preface, *Proc. NATO Adv. Res. Workshop Nonthermal Plasma Tech. Poll. Control*, Cambridge Univ. (1992), p. 13.